Eur. J. Mineral.
2004, **16**, 891-897

Interlayer structure in aspidolite, the Na analogue of phlogopite

TOSHIHIRO KOGURE[1]*, YASUYUKI BANNO[2] and RITSURO MIYAWAKI[3]

[1]Department of Earth and Planetary Science, Graduate School of Science, The University of Tokyo, 7-3-1 Hongo, Bunkyo-ku, Tokyo, 113-0033, Japan
[2]Institute of Geoscience, Geological Survey of Japan, AIST, 1-1-1 Higashi, Tsukuba, Ibaraki, 305-8567, Japan
[3]Department of Geology, The National Science Museum, 3-23-1 Hyakunin-cho, Shinjuku-ku, Tokyo, 169-0073, Japan

Abstract: It has been found that aspidolite, the Na analogue of phlogopite, has an unusual interlayer structure for micas. The aspidolite investigated is interleaved with phlogopite in a thermally metamorphosed rock. Electron microprobe chemical analyses showed similar compositions for aspidolite and phlogopite except interlayer cations of sodium and potassium. High-resolution transmission electron microscopy (HRTEM) revealed that the direction of the intralayer shift (shift between the two tetrahedral sheets in a 2:1 layer) is uniform, $a/3$ toward $[\bar{1}00]$, for all 2:1 layers, and that sodium and potassium are resolved to different interlayer regions to form interstratification of the two micas at monolayer level. HRTEM and electron diffraction analyses indicate a large layer offset, *i.e*., lateral shift between the two tetrahedral sheets across the sodium-bearing interlayer region. The amount of the layer offset is about 0.9 Å (*ca*. $a/6$) and the direction is one of $[\bar{1}00]$, [110] and $[1\bar{1}0]$. These directions are occasionally disordered. By combination of the intralayer shift and layer offset, the ordered aspidolite has different one-layer structures with monoclinic ($[\bar{1}00]$ layer offset) and triclinic ([110] or $[1\bar{1}0]$ layer offset) cells. The proposed cell dimensions are $a = 5.30$, $b = 9.18$, $c = 10.12$ Å, $\beta = 105.3°$ for the monoclinic ($C2/m$) cell and $a = 5.30$, $b = 9.18$, $c = 9.88$ Å, $\alpha = 94.4$, $\beta = 97.8$, $\gamma = 90°$ for the triclinic ($C\bar{1}$) cell. Both structures were identified in powder X-ray diffraction patterns and probably the triclinic structure is more common. This is the first report that structural variations are generated in micas by the combination of the intralayer shift and layer offset.

Key-words: mica, sodium mica, aspidolite, phlogopite, layer offset, HRTEM.

Introduction

Mica is a common mineral group with diverse compositions and origins. The basic structure of micas consists of 2:1 or *TOT* (tetrahedral-octahedral-tetrahedral) layers, and interlayer cations between the adjacent 2:1 layers (Rieder *et al*., 1998). The two tetrahedral (*T*) sheets in a 2:1 unit layer are laterally shifted by about $a/3$ (intralayer shift) to form octahedral sites between them. As six directions are possible for the intralayer shift, micas appear in several different polytypes by the choice and combination of these directions. On the other hand, the two *T* sheets belonging to different 2:1 layers across the interlayer region are hardly staggered because the interlayer cations are accommodated in the cavities formed with the two opposing tetrahedral six-fold rings. Accurate structure analyses of micas revealed that the two *T* sheets across the interlayer region are slightly shifted in real mica structures (termed "layer offset" by Bailey (1984)), but the amount of the shift is a few percent of the *a*-axis length at most (Bailey, 1984; Brigatti & Guggenheim, 2002). Consequently, the lateral displacement between the adjacent 2:1 layers in micas is almost identical with the intralayer shift. By contrast, pyrophyllite and talc, in which no interlayer cations exist, have a considerable amount of shift (close to $a/3$) between the *T* sheets across the interlayer region to reduce repulsion between opposing basal oxygen atoms and tetrahedral cations (Evans & Guggenheim, 1988).

The most common element for the interlayer cations in micas is potassium but sodium or divalent large cations can replace it. For instance, paragonite is the sodium analogue of muscovite. A number of analyses confirmed that the interlayer structure in paragonite is almost the same as that in muscovite, although the basal spacing is considerably decreased (*ca*. 0.3 Å) due to a smaller ionic radius of sodium than that of potassium (*e.g*. Sidorenko *et al*., 1977; Lin & Bailey, 1984). In contrast, few works have been reported for the structures of sodium-bearing trioctahedral micas (Spear *et al*., 1981; Oberti *et al*., 1993). Aspidolite, the Na analogue of phlogopite, was described by Schreyer *et al*. (1980) and Costa *et al*. (2001), but only its occurrence and chemistry were reported.

*E-mail: kogure@eps.s.u-tokyo.ac.jp

0935-1221/04/0016-0891 $ 3.15
DOI: 10.1127/0935-1221/2004/0016-0891

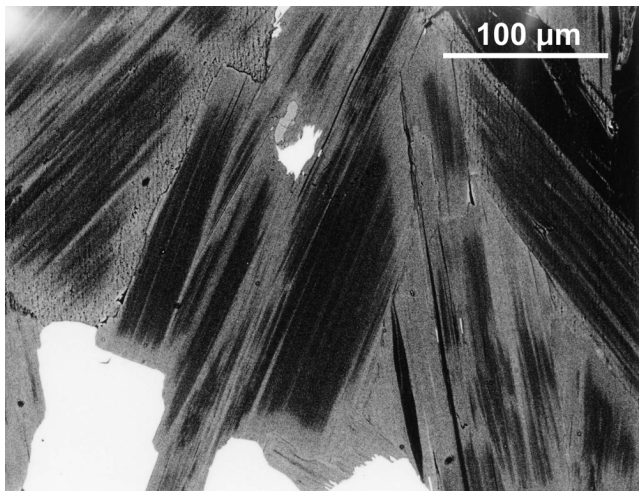

Fig. 1. Back-scattered electron image of interleaved phlogopite-aspidolite in a petrographic thin section. The dark and light contrasts correspond to sodium- and potassium-bearing compositions respectively, which was identified by X-ray chemical mapping.

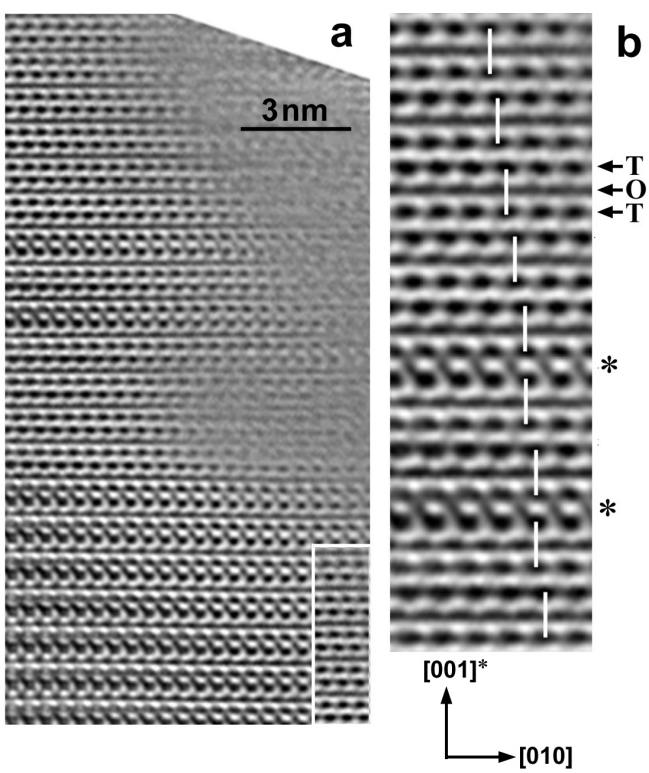

Fig. 2. (a) Filtered HRTEM image of the mica recorded down [100], showing interstratification of two kinds of layers. The inset at the bottom-right is a portion of the image near the top to indicate the different basal spacings between the two kinds of layers. (b) Magnified image near the center of (a). "T" and "O" indicate the positions of tetrahedral and octahedral sheets respectively. The white bars connect the dark spots at the upper and lower tetrahedral sheets in a 2:1 layer. Note the two tetrahedral sheets across the interlayer regions except those with asterisks are staggered. The interlayer regions marked with asterisks are interpreted to be potassium-occupied regions.

We investigated the structure of aspidolite that is interleaved with phlogopite in a thermally metamorphosed rock, by X-ray diffraction (XRD). However, the obtained diffraction patterns could not be interpreted with the aspidolite structure similar to that of phlogopite. Therefore the specimen was examined by TEM, which resulted in the discovery of a large layer offset at the interlayer regions occupied by sodium. Furthermore, it was found that this large offset leads to a new structural variation in the mica structure.

Samples and methods

Aspidolite-phlogopite interleaved mica was found in a rock sample (a registered specimen of the Geological Survey of Japan, GSJ M 35151-1) from a granitic contact aureole in Kasuga-mura, Gifu-Prefecture, central Japan. The rock is mainly composed of mica, amphibole (pargasite-magnesiosadanagaite), calcite, scapolite, titanite and apatite (Banno *et al*., 2004). In back-scattered electron (BSE) images of a petrographic thin section, the mica has distinct contrast due to segregation of potassium (phlogopite) and sodium (aspidolite), as shown in Fig. 1. Electron microprobe analyses selecting areas with uniform contrast in the BSE images showed that the composition for aspidolite (the average of five data at different areas) is $(Na_{1.77}K_{0.22})(Mg_{4.53}Al_{0.84}Fe_{0.47}Ti_{0.09})(Si_{5.11}Al_{2.89})O_{20}F_{0.07}(OH)_{3.93}$, assuming that all the iron is divalent and that aluminum is distributed to make the number of tetrahedral cations in the formula to be eight. Although the sodium-potassium ratio is considerably varied, the compositions of octahedral and tetrahedral cations are very uniform among the analyzed areas; the standard deviation of the figures in the formulae is less than 5 % of each figure. The composition for phlogopite areas is almost the same except alkali ions. The considerable fluctuation of the sodium-potassium ratio is probably due to the fine interstratification of aspidolite and phlogopite at monolayer level as described later, which hardly contributes to the contrast in the BSE images. The above composition is near the midpoint of aspidolite ($NaMg_3AlSi_3O_{10}(OH)_2$) – preiswerkite ($NaMg_2AlAl_2Si_2O_{10}(OH)_2$) series formed by Tschermak substitution, but slightly close to aspidolite. Hence this sodium mica should be called aluminian aspidolite (Rieder *et al.*, 1998).

Specimens for TEM examination along [*hk*0] directions were prepared by using the method described in Kogure (2002). Platy mica crystals picked from the rock were embedded with epoxy resin between two glass slides. After hardening, the glass slides were cut using a diamond wheel to laths of about 1 mm thickness. The laths were thinned down to about 50 μm by mechanical grinding and finished by argon ion milling. HRTEM examination was performed at 200 kV using a JEOL JEM-2010 with a nominal point resolution of 2.0 Å (C_s = 0.5 mm). High-resolution images were recorded on films at near Scherzer defocus. Successful images recorded on the films were digitized using a CCD camera for image processing. Noisy contrast from amorphous materials on the specimen surfaces was

removed using the rotational filtering technique (Kilaas, 1998) implemented with Gatan DigitalMicrograph version 2.5 (with respect to the performance of the filtering, see Kogure & Banfield, 1998).

Mica fragments of a few hundreds micrometers in lateral size and less then ten micrometers in thickness were attached to a thin glass fiber for XRD measurements. XRD patterns were obtained with a Gandolfi camera of 114.6 mm in diameter employing Ni-filtered Cu$K\alpha$ radiation. The patterns were recorded on an imaging plate and processed with a Fuji BAS-2500 bio-imaging analyzer and with a computer program by Nakamuta (1999).

Results and discussion

Layer offset in aspidolite

Figure 2 shows a filtered HRTEM image of the specimen, recorded with the electron beam parallel to [100]. Our previous works, *e.g*. Kogure (2002) can be referred to for the interpretation of the HRTEM images of micas. It is noticed that the contrast of the layers near the bottom and top of Fig. 2a are clearly different. The contrast near the bottom is the same as that of normal trioctahedral micas (see Fig. 2 in Kogure, 2002). If the crystal is sufficiently thin (< 10 nm) and the focus is adjusted to near Scherzer defocus (*ca*. – 40 nm in the present study), the contrast of the trioctahedral micas appears as follows: *T* sheet appears as distinct dark spots separated from each other by *b*/2 along the *b*-axis. This dark spot corresponds to two tetrahedra, or a tetrahedral chain extending along [100] direction. On the other hand, the octahedral (*O*) sheet is imaged as a continuous line of dark contrast (Fig. 2b). The structure near the bottom in Fig. 2a has one-layer periodicity and the two *T* sheets in a 2:1 layer are not staggered, indicating phlogopite-1*M* observed along [100] (the intralayer shift is parallel to the electron beam). The contrasts at the two *T* sheets across the interlayer regions are also not staggered, in accordance with the normal phlogopite structure where the layer offset is negligible.

On the other hand, the structure around the top of the figure has also no stagger between the two *T* sheets in a 2:1 layer, but the *T* sheet at the bottom of each layer is considerably staggered to the left from the *T* sheet at the top of the lower layer. We conclude that these interlayer regions with the large stagger between the opposing *T* sheets are occupied by sodium from the following results. First, X-ray chemical analysis by TEM-EDS (Energy Dispersive Spectroscopy) detected only sodium and potassium at the staggered and non-staggered regions, respectively. Secondly, if we cut a portion of the image at the staggered region and paste it on the non-staggered region, it is recognized that the basal spacing of the staggered layers is slightly narrow, as shown in Fig. 2a. Careful examination indicates that the decrease of the basal spacing is about 3 % or 0.3 Å, almost the same as the difference of the spacing between muscovite and paragonite (Brigatti & Guggenheim, 2002). This result also suggests that potassium and sodium are almost completely resolved into different interlayer regions and form interstratification of phlogopite and aspidolite.

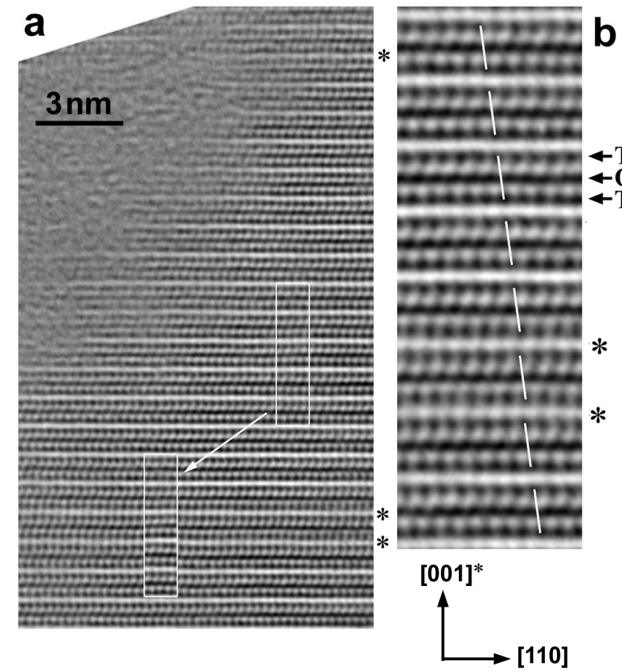

Fig. 3. (a) Filtered HRTEM image of the mica recorded down [3$\bar{1}$0]. The interlayer regions with asterisks are occupied by potassium, which is confirmed by the larger basal spacing as shown in the figure. (b) Magnified image of a portion in (a). The two potassium interlayer regions are indicated with asterisks. Note the two tetrahedral sheets across the interlayer regions are slightly staggered except those with asterisks.

Figure 3 shows a HRTEM image recorded after rotating the specimen about ***c**** by 30° in the TEM (the beam direction is [310] or [3$\bar{1}$0]). HRTEM images along these directions show that individual tetrahedra and octahedra are resolved and appear as dark spots separated by *a*/2 in the *T* and *O* sheets (Kogure, 2002). A few potassium interlayer regions (marked with asterisks in the figure) are identified with their slightly larger basal spacing. The inclined white bars in Fig. 3b connect between the closest two dark spots at the upper and lower *T* sheets in a 2:1 layer. These bars correspond to projections of the intralayer vectors connecting the two centers of the tetrahedral six-fold rings in the upper and lower *T* sheets (Kogure & Nespolo, 1999). As shown in Fig. 3b, two *T* sheets at sodium interlayer regions are slightly staggered also in this image.

Although it is possible to roughly estimate the amount and the direction of the layer offset from these HRTEM images, more quantitative estimation can be made using diffraction techniques. Figure 4 shows selected-area diffraction (SAD) patterns from an aspidolite region. The two patterns were obtained from the same area but the specimen is rotated by 30° about the ***c****-axis. If we assume that the beam directions in Fig. 4a and 4b are down [100] (0*kl* reciprocal lattice net) and [3$\bar{1}$0] (*h*·3*h*·*l* reciprocal lattice net) respectively, a triclinic C-centered cell ($C\bar{1}$) with cell parameters of a = 5.30, b = 9.18, c = 9.88 Å, α = 94.4, β = 97.8, γ = 90° is deduced. Actually these figures

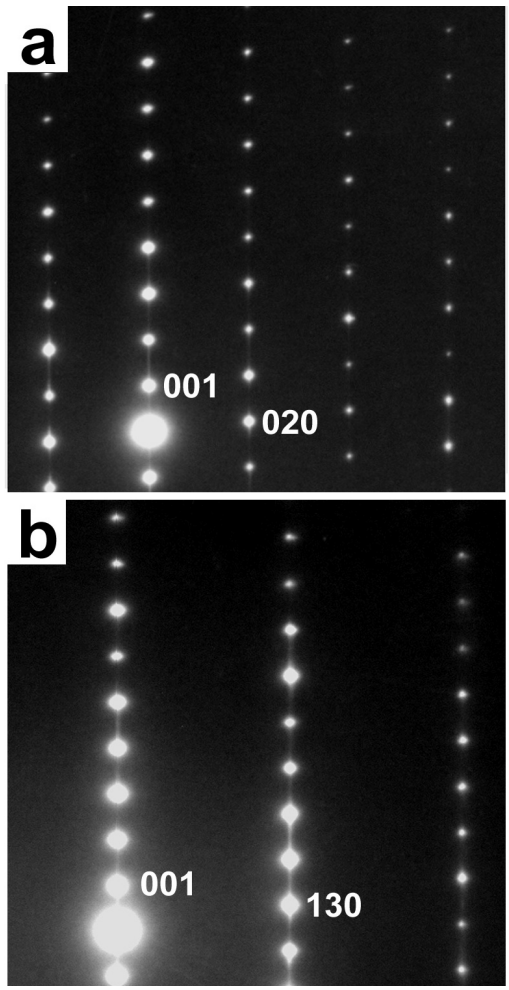

Fig. 4. Selected-area electron diffraction patterns from aspidolite, with the electron beam down (a) [100] and (b) [3$\bar{1}$0].

have been refined from peak positions in XRD patterns as described below, but their standard deviations could not be calculated due to the limited number of non-overlapped peaks in the pattern. The lateral displacement between adjacent layers calculated from these cell parameters is $-0.253\boldsymbol{a} - 0.083\boldsymbol{b}$. If we assume that the intralayer shift in aspidolite is exactly $-\boldsymbol{a}/3$ as that in phlogopite-1*M*, the layer offset at the interlayer region is $0.080\boldsymbol{a} - 0.083\boldsymbol{b}$. In other words, the amount of the layer offset is 0.9 Å and the direction of the offset is almost [1$\bar{1}$0]. Such a large layer offset (about one sixth of the *a*-length) has been once reported in a trioctahedral sodium mica, $NaMg_3(Si_{3.5}Mg_{0.5})O_{10}(OH)_2$ synthesized from talc (Drits *et al*., 1979; Drits, 1987), although the amount of the offset was close to *a*/3 in their case.

Figure 5 illustrates the proposed interlayer structure in aspidolite. The atomic coordinates for *T* sheets were adopted from those of aluminian phlogopite (Phl3a) in Alietti *et al.* (1995), because the composition for the 2:1 layer is almost the same as that of our specimen. The position of sodium ions is assumed to be the center of the staggered two tetrahedral rings. The direction of the offset in aspidolite is the same as those found in pyrophyllite and talc (Evans & Guggenheim, 1988), and in paragonite (Lin & Bailey, 1984); they are shifted from each other as an apex oxygen atom of the ditrigonal oxygen ring is separated from the center of the cavity (Fig. 5). As mentioned above, large repulsive force between the opposing *T* sheets across the interlayer region is expected but the lateral shift (layer offset) between the two *T* sheets is blocked by interlayer cations in the cavity space. However, if the size of the interlayer cations is small compared to the cavity space, the layer offset can occur just like in pyrophyllite and talc although the amount of the offset is limited by existence of the interlayer cations (notice the amount of the offset in aspidolite is about half of that in talc). However, previous works reported that sodium micas do not always posses a large layer offset. The amount of the layer offset in paragonite is about one fourth of that in aspidolite (Lin & Bailey, 1984). Preiswerkite, $NaMg_2AlSi_2Al_2O_{10}(OH)_2$, does not posses layer offset (Oberti *et al*., 1993). This difference is related to the ditrigonal rotation angle (α_t) in *T* sheets that primarily determines the cavity space in the tetrahedral six-

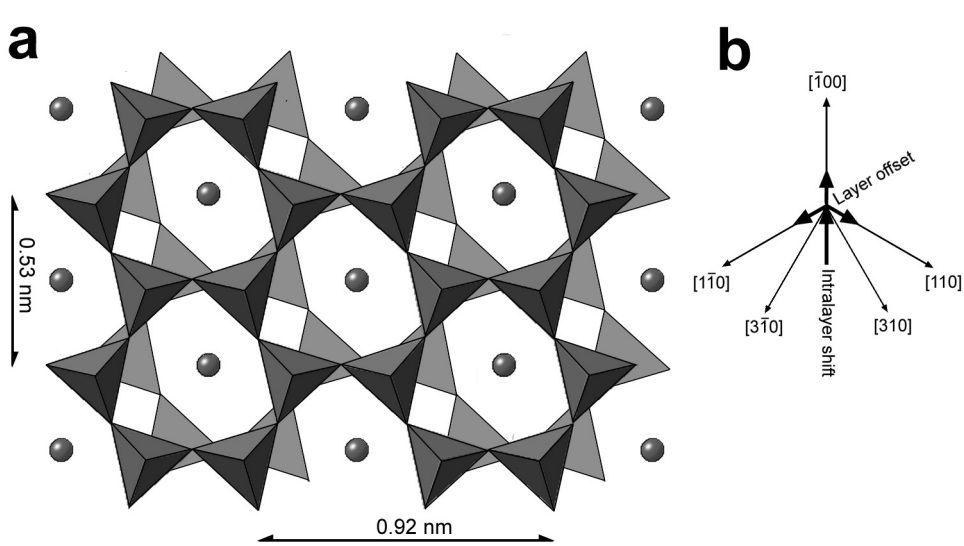

Fig. 5. (a) Schematic figure for the interlayer structure in aspidolite, showing two tetrahedral sheets and sodium ions between them. The tetrahedral sheets were drawn with the atomic coordinates by Alietti *et al*. (1995), and the two sheets were staggered by 0.9 Å along [1$\bar{1}$0]. Sodium ions are assumed to exist at the center of the staggered six-fold rings above and below the sodium ions. (b) Diagram to show the relationship between the intralayer shift ($-\boldsymbol{a}/3$) and the layer offsets along the three directions (see the text).

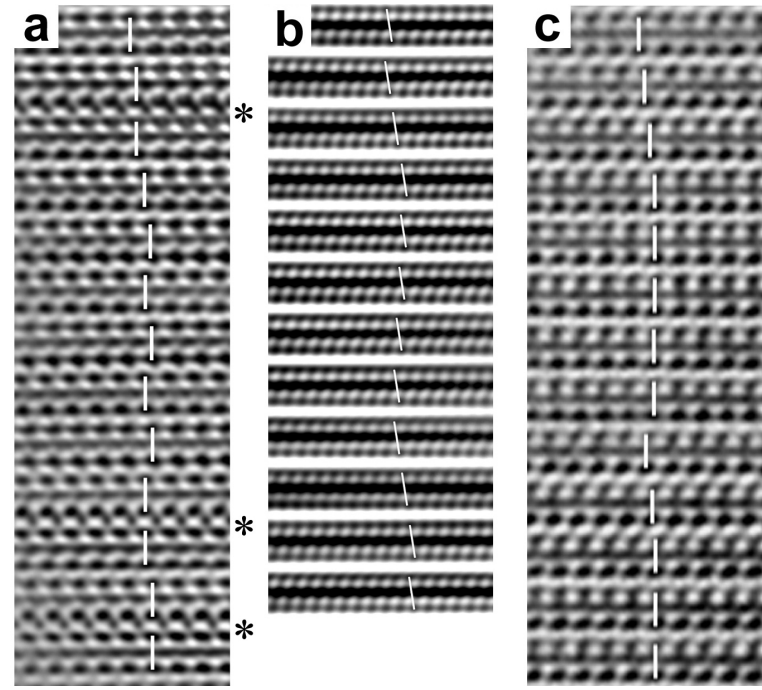

Fig. 6. (a) Filtered HRTEM image recorded down [100] where a random mixture of the left- and right-hand staggers at the interlayer regions is observed. The interlayer regions with the asterisk are occupied by potassium. (b) Filtered HRTEM image of aspidolite recorded down [$\bar{3}$10]. Two kinds of staggers at the interlayer regions are observed. (c) Filtered HRTEM image of aspidolite recorded down [100]. Note many non-staggered interlayer regions are observed (see the text).

fold ring. The ditrigonal rotation is formed to compensate the mismatch of lateral dimensions between *T* and *O* sheets (Ferraris & Ivaldi, 2002). Although α_t in aspidolite is unknown, it must be close to that in the coexisting phlogopite because their 2:1 layers have the same composition and the two micas are coherently interstratified as in Fig. 2 and 3. α_t in a phlogopite with similar composition (aluminian phlogopite by Alietti *et al.*, 1995) is 12.5°, considerably smaller than that in paragonite (*ca*.16° in the table by Brigatti & Guggenheim, 2002) and preiswerkite (20°) (Oberti *et al*., 1993). In conclusion, the large amount of the layer offset in aspidolite is reasonable, if we assume a small α_t in the 2:1 layer and the resultant large cavity space in this mica.

Structural variation in aspidolite by the layer offset

As a pseudo three-fold axis runs through the center of the tetrahedral six-fold ring, it is expected that the layer offset occurs not only along [1$\bar{1}$0], but also along [110] and [$\bar{1}$00]. These different directions of the layer offset were readily found in HRTEM images (Fig. 6). In Fig. 6a, a random mixture of staggers to left and right is observed. If these two kinds of staggers come from the layer offsets along [1$\bar{1}$0] and [110], the two offsets must be observed as different amounts and directions of staggers in the images down [310] or [3$\bar{1}$0] (Fig. 5b). Fig. 6b is a HRTEM image recorded down [3$\bar{1}$0], where two kinds of staggers, a large amount to the right and a small amount to the left are distinguished. It is found that the direction of the larger stagger is opposite to the inclination of the white bars that correspond to the projection of the intralayer shift. This agrees with the diagram in Fig. 5b. Furthermore, some interlayer regions show no stagger although their basal spacing is the same as that of staggered layers (Fig. 6c). One may suspect that the non-staggered interlayer regions correspond to the normal mica structure with negligible layer offset, but it is more reasonable to suggest that they are [$\bar{1}$00] layer offset. Recording two HRTEM images at the same area along the different directions, which is effective to analyze three-dimensional stacking structures in micas (Kogure & Nespolo, 1999), was not successful because the phlogopite and aspidolite were too beam-sensitive to record two HR images from the same area. However, an XRD pattern as described later clearly indicates the existence of the [$\bar{1}$00] layer offset. In this case the direction of the layer offset and intralayer shift is the same, which results in a monoclinic unit cell. If the amount of the layer offset to [$\bar{1}$00] is the same as that to [1$\bar{1}$0], the cell parameters are a = 5.30, b = 9.18, c = 10.12 Å, β = 105.3° and the space group is *C*2/*m*.

Figure 7 shows XRD patterns from the mica fragments obtained using a Gandolfi camera, and calculated patterns from the proposed structures for comparison. Background of the observed patterns was subtracted by using proper exponential functions. The calculated pattern for phlogopite-1*M* was derived using the crystal parameters for the aluminian phlogopite (Phl3a) in Alietti *et al*. (1995) because of the similar chemical composition. The atomic coordinates for aspidolite were derived assuming the same 2:1 layer as that in the aluminian phlogopite, the decreased interlayer separation by 0.35 Å (determined from the peak positions of the basal reflections), the layer offset as described above (note that the [1$\bar{1}$0] and [110] offsets generate the same crystal structure if ordered), and sodium atoms at the center of the staggered two tetrahedral six-fold rings (Fig. 5a). A pseudo-Voight function (the same ratio of Gauss and Lorentz functions) with a half-width of 0.25° was assumed for the peak profile. Figure 7a indicates that all major peaks in the observed pattern can be explained

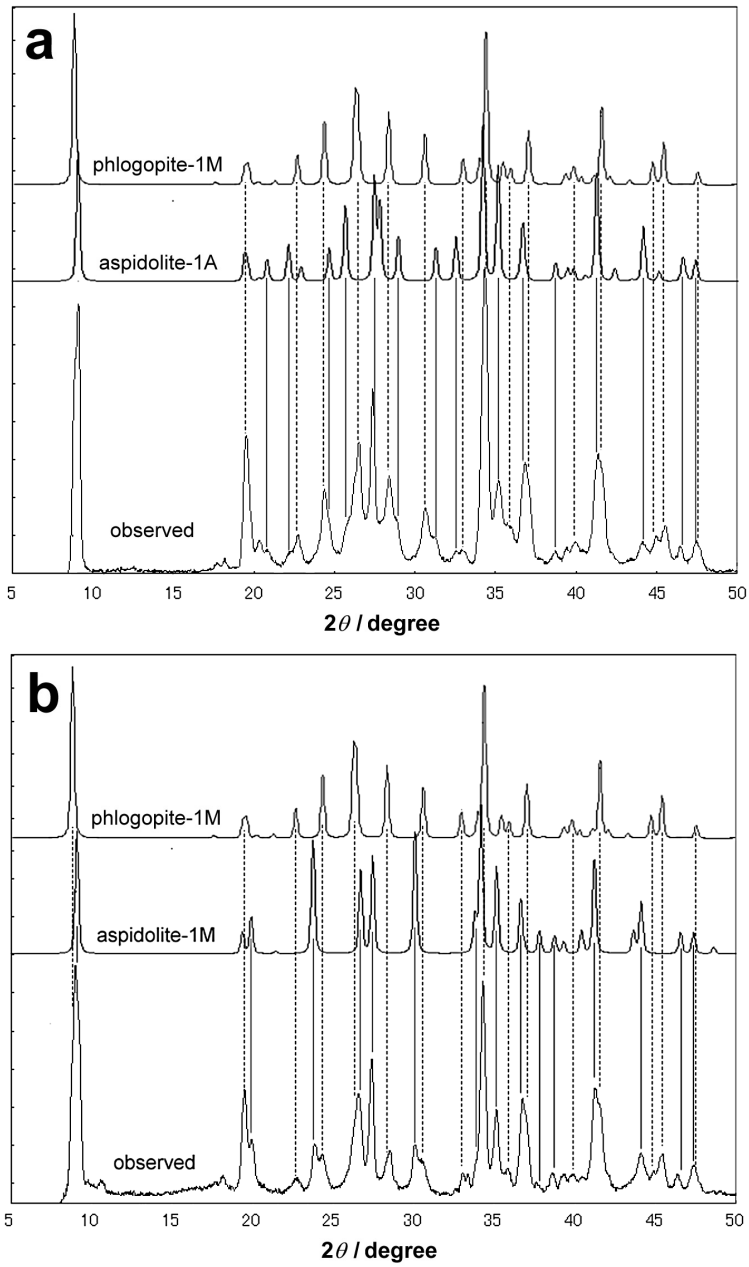

Fig. 7. (a) Orientation-averaged XRD pattern from a mica fragment acquired with a G andolfi camera, and calculated powder diffraction patterns for phlogopite-1*M* and aspidolite-1*A*. See the text for the detail of the calculation. (b) Diffraction pattern from another fragment and calculated patterns for phlogopite-1*M* and aspidolite-1*M*.

with the phlogopite-1*M* and the triclinic aspidolite (aspidolite-1*A*). Figure 7b shows the observed diffraction pattern from another fragment, where several new peaks that do not exist in Figure 7a are observed. These peaks are only explained by the monoclinic ([$\bar{1}$00] layer offset) aspidolite with the large β angle (aspidolite-1*M*). These XRD results confirm the existence of the structural variations in the sodium mica. In addition, it is noteworthy that they can be identified also in XRD, not only in TEM micrographs from narrow areas. Three more mica fragments were measured and they showed XRD patterns similar to that in Fig. 7a (phlogopite-1*M* and aspidolite-1*A*). From this result and TEM examination, probably the triclinic structure is more common than the monoclinic one.

These two structural variations in aspidolite can be called polytypes according to the official definition of polytypism (Guinier *et al*., 1984), if the direction of the layer offset is ordered. However, this polytypism in aspidolite is an exceptional one among micas and most phyllosilicates for which the structural variations are generated with interlayer shifts with the amount of zero, *a*/3 or *b*/3 (if idealized in some cases) to certain directions (Bailey, 1988; Ďurovič, 1992). Further discussion and research will be necessary to decide whether this layer offset is an extreme defect or a new stacking vector so far not considered in micas (S. Ďurovič & M. Nespolo, pers. comm.).

Although the occurrence of aspidolite in nature is limited, findings in the present study will raise reconsideration for the structures of other micas if large interlayer cavities and smaller interlayer cations are expected. For instance, wonesite, trioctahedral sodium-mica in which occupancy of the interlayer cations is about half, is reported

as a one-layer monoclinic cell with a relatively large β angle (103.18°) (Spear *et al*., 1981). This mica may contain a large layer offset. The structure analysis in their reports used only 00*l* reflections and is clearly incomplete to discuss its interlayer structure. Furthermore, dehydrated forms of some vermiculites or smectites can be candidates of such a new interlayer structure. HRTEM investigations like the present study should be conducted as well for these minerals.

Acknowledgements: We are grateful to T. Kamiya and S. Yamada for donating valuable specimens. We also thank Dr. M. Nespolo (Université Henri Poincaré Nancy 1, France), Dr. G. Ferraris (Università di Torino, Italy), Dr. S. Ďurovič (Slovak Academy of Science, Slovakia) and Dr. V.A. Drits (Geological Institute, Russian Academy of Sciences, Russia) for valuable discussions. Comments and suggestions by Dr. E. Tillmanns (the chief editor) and an anonymous reviewer improved the manuscript considerably. Transmission electron microscopy was carried out in the Electron Microbeam Analysis Facility of the Department of Earth and Planetary Science, the University of Tokyo.

References

Alietti, E., Brigatti, M. F., Poppi, L. (1995): The crystal structure and chemistry of high-aluminium phlogopite. *Mineral. Mag.*, **59**,149-157.

Bailey, S.W. (1984): Crystal chemistry of the true micas. *in* "Micas, *Review in Mineralogy* Vol. **13**", Mineralogical Society of America, Washington, D.C., 13-60.

Bailey, S.W. (Ed) (1988): Hydrous phyllosilicates (exclusive of micas). *Review in Mineralogy* **19**, Mineralogical society of America, Washington, D.C., 725p.

Banno, Y., Miyawaki, R., Matsubara, S., Makino, K., Bunno, M., Yamada, S., Kamiya, T. (2004): Magnesiosadanagaite, a new member of the amphibole group from Kasuga-mura, Gifu Prefecture, central Japan. *Eur. J. Mineral.*, **16**, 177-183.

Brigatti, M.F. & Guggenheim, S. (2002): Mica crystal chemistry and the influence of pressure, temperature, and solid solution on atomistic models. *in* "Micas: Crystal Chemistry & Metamorphic Petrology, Reviews in Mineralogy and Geochemistry Vol. **46**", A. Mottana, F.P. Sassi, J.B. Thompson, JR., S. Guggenheim, ed. Mineralogical Society of America, Washington, D.C., 1-98.

Costa, F., Dungan, M.A., Singer, B.S. (2001): Magmatic Na-rich phlogopite in a suite of gabbroic crustal xenoliths from Volcán San Pedro, Chilean Andes: Evidence for a solvus relation between phlogopite and aspidolite. *Am. Mineral.*, **86**, 29-35.

Drits, V.A. (1987): Electron diffraction and high-resolution electron microscopy of mineral structures. Springer-Verlag, Berlin, 304p.

Drits, V.A., Kotytkova, E.N., Dmitrik, A.L., Alexandrova, V.A. (1979): Mica $NaMg_3(Si_{3.5}Mg_{0.5})O_{10}(OH)_2$ with the layer super cell and talc-like layer stacking. *in* "Cation ordering in mineral structures", I.L. Lapides, ed. Publisher Nauka, Novosibirsk, 128-151 (in Russian).

Ďurovič, S. (1992): Layer stacking in general polytypic structures. *in* "International Tables for Crystallography Vol. C", A.C.J. Wilson, ed. Kluwer Academic Publishers, Dordrecht, Netherlands, 667-680.

Evans, B.W. & Guggenheim, S. (1988): Talc, pyrophyllite, and related minerals. *in* "Hydrous Phyllosilicates (exclusive of micas), Review in Mineralogy Vol. **19**", Mineralogical Society of America, Washington, D.C., 225-294.

Ferraris, G. and Ivaldi, G. (2002): Strcutural features of micas. *in* "Micas: Crystal Chemistry & Metamorphic Petrology, Reviews in Mineralogy and Geochemistry Vol. **46**", A. Mottana, F.P. Sassi, J.B. Thompson, JR., S. Guggenheim, ed. Mineralogical Society of America, Washington, D.C., 117-153.

Guinier, A., Bokij, G.B., Boll-Dornberger, K., Cowley, J.M., Ďurovič, S., Jagodzinski, H., Krishna, P., De Wolff, P.M., Zvyagin, B.B., Cox, D.E., Goodman, P., Hahn, Th., Kuchitsu, K., Abrahams, S.C. (1984): Nomenclature of polytype structures. Report of the International Union of Crystallography Ad-Hoc committee on the nomenclature of disordered, modulated and polytype structures. *Acta Cryst.*, **A40**, 399-404.

Kilaas, R. (1998): Optical and near-optical filters in high-resolution electron microscopy. *J. Microscopy*, **190**, 45-51.

Kogure, T. (2002): Investigation of micas using advanced TEM. *in* "Micas: Crystal Chemistry & Metamorphic Petrology, Reviews in Mineralogy and Geochemistry Vol. **46**", A. Mottana, F.P. Sassi, J.B. Thompson, JR., S. Guggenheim, ed. Mineralogical Society of America, Washington, D.C., 281-312.

Kogure, T. & Banfield, J.F. (1998): Direct identification of the six polytypes of chlorite characterized by semi-random stacking. *Am. Mineral.*, **83**, 925-930.

Kogure, T. & Nespolo, M. (1999): First occurence of a stacking sequence with (± 60°, 180°) rotation in Mg-rich annite. *Clays Clay Minerals*, **47**, 784-792.

Lin, C-Y. & Bailey, S.W. (1984): The crystal structure of paragonite-$2M_1$. *Am. Mineral.*, **69**, 122-127.

Oberti, R., Ungaretti, L., Tlili, A., Smith, D.C., Robert, J-L. (1993): The crystal structure of preiswekite. *Am. Mineral.*, **78**, 1290-1298.

Nakamuta, Y. (1999): Precise analysis of a very small mineral by an X-ray diffraction method. *J. Mineral. Soc. Jpn.*, **28**, 117-121 (in Japanese with English abstract).

Rieder, M., Cavazzini, G., D'yakonov, Yu.S., Frank-Kamenetskii, V.A., Gottardi, G., Guggenheim, S., Koval', P.V., Müller. G., Neiva, A.M.R., Radoslowich, E.W., Robert, J.L., Sassi, F.P., Takeda, H., Weiss, Z., Wones. D.R. (1998): Nomenclature of the micas. *Can. Mineral.*, **36**, 905-912.

Schreyer, W., Abraham, K., Kulke, H. (1980): Natural sodium phlogopite coexisting with potassium phlogopite and sodian aluminian talc in a metamorphic evaporite sequence from Derrag, Tell Atlas, Algeria. *Contrib. Mineral. Petrol.*, **74**, 223-233.

Sidorenko, O.V., Zvyagin, B.B., Soboleva, S.V. (1977): Refinement of the crystal structure of $2M_1$ paragonite by the method of high-voltage electron diffraction. *Sov. Phys. Crystallogr.*, **22**, 554-556.

Spear, F.S., Hazen, R.M. Rumble, D. (1981): Wonesite: a new rock-forming silicate from the Post Pond Volcanics, Vermont. *Am. Mineral.*, **66**, 100-105.

Received 12 February 2004
Modified version received 1 June 2004
Accepted 28 June 2004